# A Systematic Survey of Carbonic Anhydrase mRNA Expression During Mammalian Inner Ear Development

**Ling Wu,[1,2,3] Borum Sagong,[4] Jae Young Choi,[1,3] Un-Kyung Kim,[4] and Jinwoong Bok[1,2,3]***

**Background: Carbonic anhydrases (CAs), which catalyze $CO_2$ hydration to bicarbonate and protons, have been suggested to regulate potassium homeostasis and endocochlear potential in the mammalian cochlea. Sixteen mammalian CA isozymes are currently known. To understand the specific roles of CA isozymes in the inner ear, a systematic survey was conducted to reveal temporal and spatial expression patterns of all 16 CA isozymes during inner ear development. Results: Our quantitative reverse transcriptase-polymerase chain reaction results showed that different tissues express unique combinations of CA isozymes. During inner ear development, transcripts of four cytosolic isozymes (*Car1*, *Car2*, *Car3*, and *Car13*), two membrane-bound isozymes (*Car12* and *Car14*), and two CA-related proteins (*Car8* and *Car11*) were expressed at higher levels than other isozymes. Spatial expression patterns of these isozymes within developing inner ears were determined by in situ hybridization. Each isozyme showed a unique expression pattern during development. For example, *Car12* and *Car13* expression closely overlapped with *Pendrin*, an anion exchanger, while *Car2* overlapped with Na-K-ATPase in type II and IV otic fibrocytes, suggesting functional relationships in the inner ear. Conclusions: The temporal and spatial expression patterns of each CA isozyme suggest unique and differential roles in inner ear development and function. *Developmental Dynamics 242:269–280, 2013*.** © **2012 Wiley Periodicals, Inc.**

**Key words:** carbonic anhydrase; inner ear; cochlea; mouse; development

**Key findings:**

- A systematic survey for transcripts of all 16 mammalian carbonic anhydrase isozymes in various organs showed that each organ expresses unique combinations of carbonic anhydrase isozymes.
- During inner ear development, transcripts of four cytosolic isozymes (*Car1*, *Car2*, *Car3*, and *Car13*), two membrane-bound isozymes (*Car12* and *Car14*), and two CA-related proteins (*Car8* and *Car11*) were expressed at higher levels than other isozymes.
- Each isozyme showed a unique temporal and spatial expression pattern during inner ear development.
- Expression patterns for some isozymes closely overlapped with genes previously associated with inner ear development or function, such as *Pendrin*, *Pou3f4*, or *Bmp4*.

Accepted 3 December 2012

## INTRODUCTION

Carbonic anhydrases (CAs) are zinc-containing metalloenzymes that catalyze the reversible conversion of carbon dioxide to bicarbonate ion and a proton. These enzymes, found in all types of organisms, are encoded by five independent gene families: the α-, β-, γ-, δ-, and ϵ-CAs (Supuran, 2008b;

[1]Department of Anatomy, Yonsei University College of Medicine, Seoul, South Korea
[2]Department of Otorhinolaryngology, Yonsei University College of Medicine, Seoul, South Korea
[3]BK21 Project for Medical Science, Yonsei University College of Medicine, Seoul, South Korea
[4]Department of Biology, Kyungpook National University, Daegu, South Korea
Grant sponsor: Korea Healthcare Technology R&D Project, Ministry for Health, Welfare & Family Affairs; Grant number: A100493.
Grant sponsor: Basic Science Research Program through the National Research Foundation of Korea (NRF) funded by the Ministry of Education, Science and Technology; Grant number: 2011-0028066.
***Correspondence to: Jinwoong Bok, Department of Anatomy, Yonsei University College of Medicine, Seoul, South Korea. E-mail: bokj@yuhs.ac**

**DOI: 10.1002/dvdy.23917**
Published online 10 December 2012 in Wiley Online Library (wileyonlinelibrary.com).

© **2012 Wiley Periodicals, Inc.**

Xu et al., 2008). Only α-CA family members have been identified in mammals (Henry and Swenson, 2000; Esbaugh and Tufts, 2006). Thus far, 16 α-CA isozymes have been described, with different catalytic activities and subcellular localizations: CAI, II, III, VII, and XIII are cytoplasmic; CAIV, IX, XII, XIV, and XV are membrane-bound; CAVa and Vb are mitochondrial; and CAVI is secreted (Supuran, 2008a,b). CAVIII, X, and XI are called CA-related proteins (CA-RPs) because they lack classical CA enzymatic activity and their biological functions remain unclear.

The importance of carbonic anhydrases has been shown in many physiological and pathological processes, including pH and $CO_2$ homeostasis, electrolyte secretion, respiration, $CO_2/HCO_3^-$ transport, and bone resorption and calcification (Supuran, 2008a). In the respiratory system, CAs are involved in most $CO_2$ transport and excretion from metabolically active tissues to red blood cells, and finally to gas exchanging organs, such as the lungs (Henry and Swenson, 2000). Cytoplasmic CAI and II are the most abundant CA isozymes in the red blood cells, while both cytoplasmic (CAII) and membrane-bound CAs (CAIV) are found in the lung (Henry and Swenson, 2000; Esbaugh and Tufts, 2006). The role of CAs has also been studied in detail in regulating renal physiology, such as acid/base homeostasis and bicarbonate reabsorption (Purkerson and Schwartz, 2007). CAs are expressed in most kidney segments. Cytoplasmic CAII accounts for most CA activity in the kidney, and different combinations of membrane-bound CAs, including CAIV, CAXII, CAXIV, and CAXV, are also expressed in different species (Purkerson and Schwartz, 2007). CAII is involved in bone physiology, such as osteoclast differentiation and bone resorption, and CAII-deficiency leads to osteopetrosis in humans and mice (Sly and Hu, 1995; Lehenkari et al., 1998; Margolis et al., 2008). In addition, various CAs expressed in the gastrointestinal canal and digestive glands are involved in ammonia detoxification, saliva production, gastric acid production, bile production, pancreatic juice production, and intestinal ion transport (Pan et al., 2007; Supuran, 2008a). Mitochondrial CAV has been associated with molecular signaling, such as insulin secretion in pancreatic β cells (Parkkila et al., 1998). Some CA isozymes are down- or up-regulated in various tumors and have been associated with oncogenesis and tumor progression (Supuran, 2008a,b). Consistently, two hypoxia-inducible CA isozymes, CAIX and XII, were shown to promote tumor growth by regulating pH in an acidic and hypoxic microenvironment (Jarvela et al., 2008; Chiche et al., 2009). In the brain, CAIV and XIV were shown to regulate pH in extracellular fluid (Shah et al., 2005). Lastly, CAIII, which is highly expressed in many tissues, including skeletal muscle, has relatively low CA activity. Its physiological role is unclear because mice lacking CAIII do not have noticeable anatomical or physiological abnormalities (Kim et al., 2004). CAIII can, however, protect cells from oxidative damage by S-glutathiolation on two cysteine residues in response to oxidative stress, thereby functioning as an oxyradical scavenger (Raisanen et al., 1999; Mallis et al., 2002, 2000; Gailly et al., 2008).

CA activity in the inner ears has been demonstrated biochemically by visualizing $CO_2$ hydration in guinea pigs, cats, and chinchillas (Erulkar and Maren, 1961; Lim et al., 1983; Hsu and Nomura, 1985; Okamura et al., 1996). Although the specific location of CA activity in the inner ear differs slightly depending on the species and detection method, CA activity is present in the organ of Corti, outer sulcus cells and their associated root processes, otic fibrocytes in the spiral ligament, as well as spiral ganglion neurons. Consistently, immunohistochemical studies have detected CAII and CAIII immunoreactivity in the otic fibrocytes, spiral limbus, and Reissner's membrane in gerbil, guinea pig, and human cochlea, with slight differences among species and detection methods.

The role of CA activity in the inner ear was first suggested by Erulkar and Maren (Erulkar and Maren, 1961). In cat inner ears, CA activity is distributed along the cochlear duct, with the highest concentrations in the apical turn, progressively lower concentrations toward the basal turns, and lowest concentrations in the vestibule (Erulkar and Maren, 1961). Administering intravenous acetazolamide, a specific CA inhibitor, considerably reduced the perilymph and endolymph volumes and pressures, and eliminated the high potassium concentration in the endolymph (Erulkar and Maren, 1961). Consistently, inhibiting CA activity affects the generation of endocochlear potential in guinea pigs and rats, suggesting a critical role of CA activity in the sound transduction (Prazma, 1978; Sterkers et al., 1984; Ikeda et al., 1987). Furthermore, CA activity has also been associated with normal otolith (otoconia) development in mice, chicken, and fish (Purichia and Erway, 1972; Kido et al., 1991; Tohse et al., 2004).

Despite the critical roles in the auditory and vestibular functions, no systematic study has been conducted to determine the expression patterns of all known CA isozymes in the mammalian inner ear. Although CAII and III localization have been described in some cochlear regions (Spicer and Schulte, 1991; Ichimiya et al., 1994; Weber et al., 2001), they do not account for all CA activities in the inner ear (Erulkar and Maren, 1961; Lim et al., 1983; Hsu and Nomura, 1985; Okamura et al., 1996). In this study, we examined the temporal and spatial expression of all known CA isozymes by quantitative real-time polymerase chain reaction (qRT-PCR) and in situ hybridization in mouse embryonic and postnatal inner ears. Our study provides comprehensive expression profiles for the CA isozymes and their potential role in inner ear development and function.

## RESULTS AND DISCUSSION

### Expression Profiles of Carbonic Anhydrases in Various Tissues in Mice

The expression levels of all known CA isozymes were analyzed by semi-quantitative reverse transcriptase PCR (RT-PCR) of RNAs isolated from various tissues, including inner ear, brain, kidney, and liver of 3-week-old mice (Fig. 1A). In the inner ear, transcripts of four cytosolic isozymes

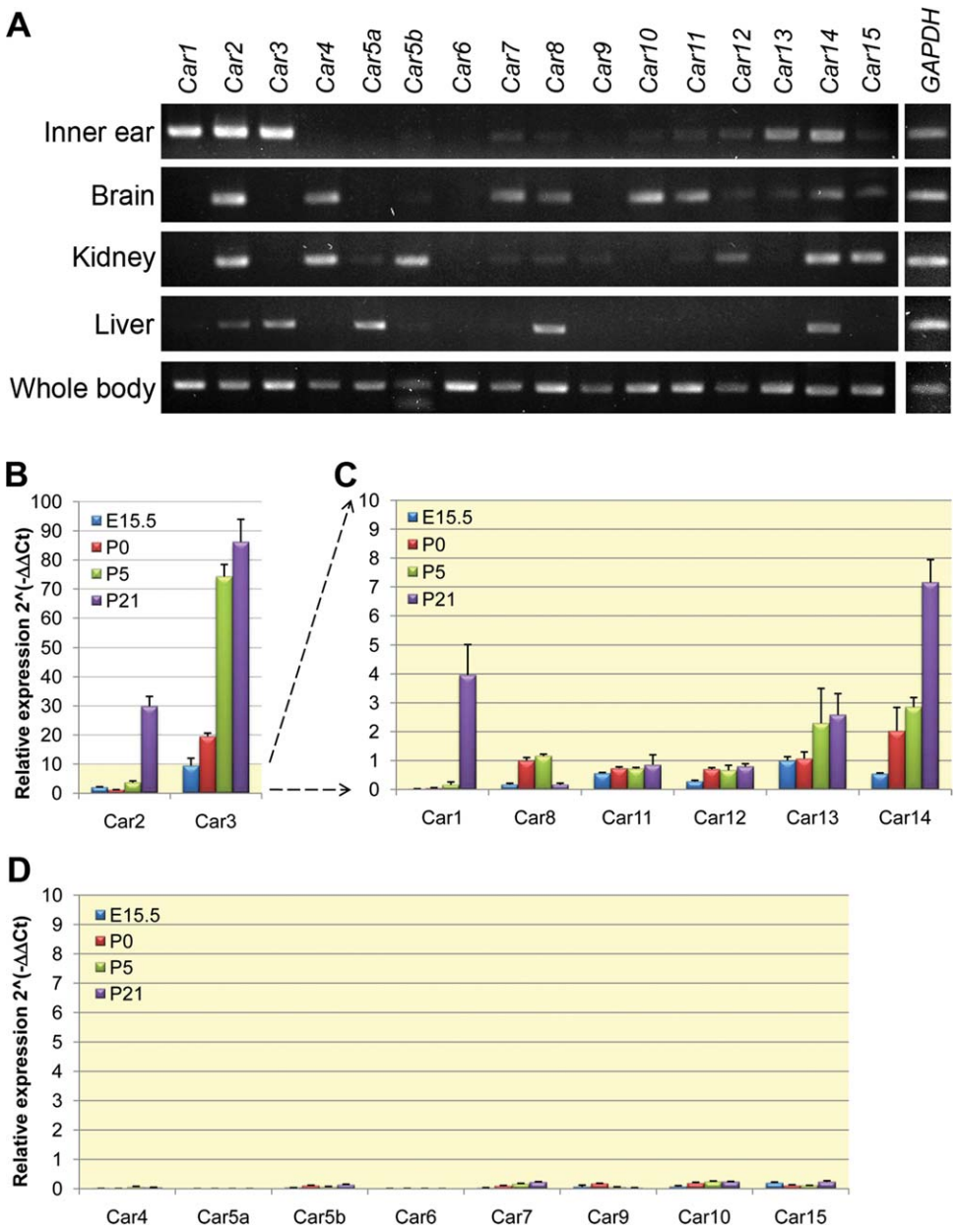


**Fig. 1.** Expression of CA transcripts in various tissues and during inner ear development. **A:** Expression of all 16 CA isozyme transcripts was analyzed by semi-quantitative reverse transcriptase-polymerase chain reaction (RT-PCR) in inner ear, brain, kidney, and liver from P21 mice. Total cDNA extracted from the whole body of postnatal day (P) 8 mouse embryo was used as a positive control. **B–D:** Temporal expression patterns of each CA isozyme during inner ear development were analyzed by quantitative real-time PCR. Please refer to the text for details.

(*Car1*, *Car2*, *Car3*, and *Car13*) and a membrane-bound isozyme (*Car14*) were expressed at higher levels than the other isozymes. In the brain, transcripts of two cytosolic isozymes (*Car2* and *Car7*) and two membrane-bound isozymes (*Car4* and *Car14*) were strongly expressed. In addition, transcripts of three acatalytic CA-related proteins (CA-RPs) (*Car8*, *Car10*, and *Car11*) were also expressed. In the kidney, transcripts of a cytosolic isozyme (*Car2*), four membrane-bound isozymes (*Car4*, *Car12*, *Car14*, and *Car15*), and a mitochondrial isozyme (*Car5b*) were expressed relatively strongly. In the liver, two cytosolic isozymes (*Car2* and *Car3*), a mitochondrial isozyme (*Car5a*), a membrane-bound isozyme (*Car14*), and a CA-RP (*Car8*), were expressed. These results showed that each tissue expresses a unique combination of CA isozymes, although some isozymes, such as *Car2* and *Car14*, appear to be ubiquitous.

## Temporal Expression of Carbonic Anhydrases During Inner Ear Development

To determine temporal expression patterns of CAs during inner ear development, we performed qRT-PCR at embryonic day (E) 15.5, postnatal day (P) 0, P5, and P21 (Fig. 1B–D). Consistent with the semi-quantitative RT-PCR (Fig. 1A), *Car1*, *Car2*, *Car3*, *Car13*, and *Car14* showed relatively high expression at P21 (Fig. 1B,C). In

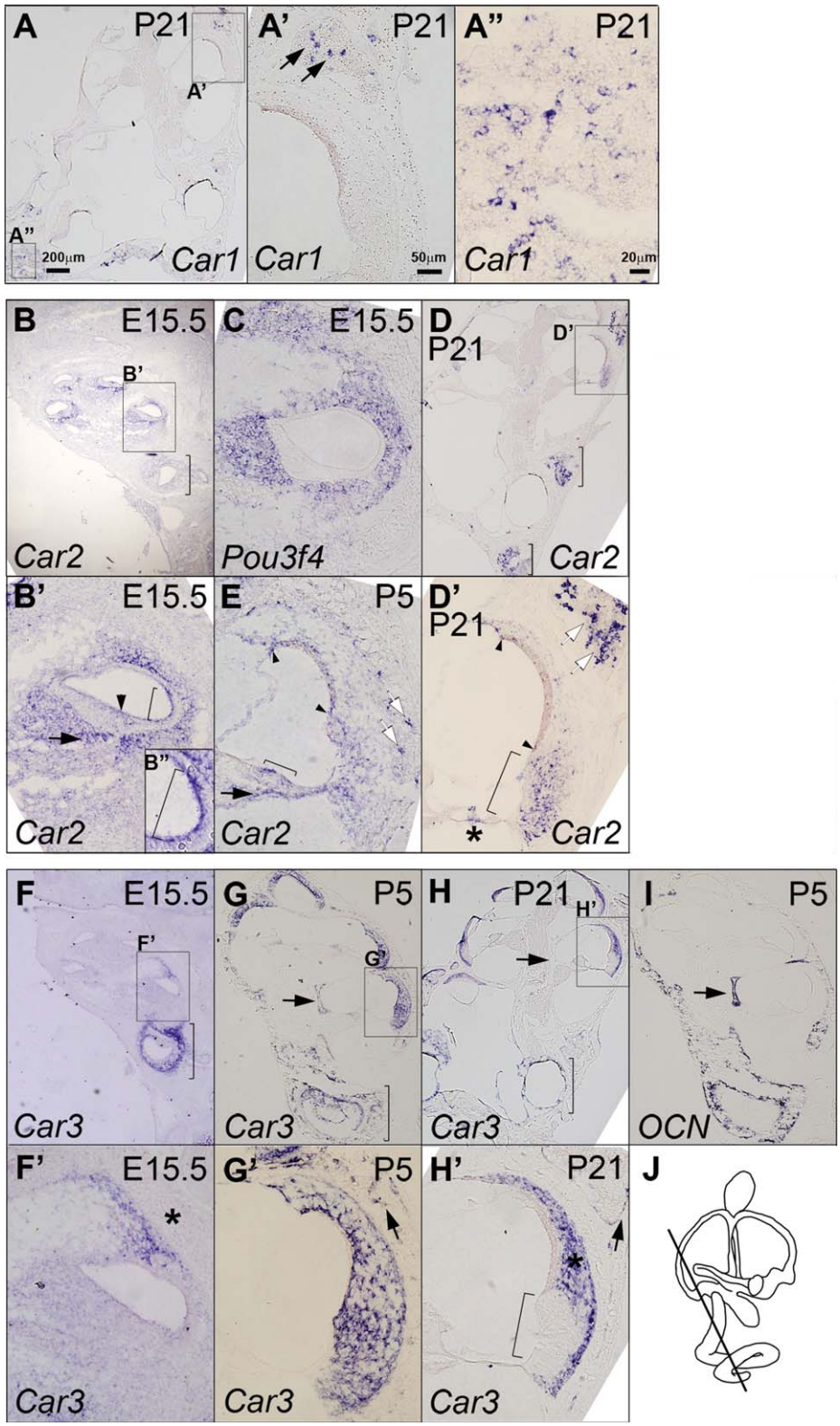


**Fig. 2.** Expression patterns of *Car1*, *Car2*, and *Car3* in the developing mouse inner ear. **A:** *Car1* was expressed in bone marrow of the otic capsule in the cochlea (A′, arrows) and vestibule (A″) at P21. **B:** At embryonic day (E) 15.5, *Car2* was expressed in the mesenchyme surrounding the cochlea and vestibule (bracket), but not in the entire periotic mesenchyme, indicated by *Pou3f4* expression **C:**. Weak epithelial expression was found in the outer sulcus (B′, B″, bracket), GER (arrowhead), and basilar membrane (arrow). **E:** At postnatal day (P) 5, *Car2* was weakly expressed in otic fibrocytes, stria vascularis (arrowheads), otic capsule (white arrows), basilar membrane (black arrow), and inner sulcus (bracket). **D:** At P21, *Car2* was strongly expressed in type II and IV fibrocytes (D′, bracket) and bone marrow (D, bracket; D′, white arrows). *Car2* was also weakly expressed in type I fibrocytes and the organ of Corti, likely in the outer hair cells (D′, asterisk). **F:** *Car3* was initially expressed near the presumptive stria vascularis at E15.5 (F,F′, asterisk), expanded to the entire spiral ligament at P5 (G,G′), and restricted to type I, III, and V fibrocytes at P21 (H,H′, asterisk). *Car3* expression was also found in the otic capsule (G,H, brackets) and modiolus (G, arrow), which is comparable to *Osteocalcin* (*OCN*) (I, arrow). Scale bar in A applies to B,D, and F–I; the scale bar in A′ applies to B′, D′, E, and F′–H′; the scale bar in A″ applies to B″.

addition, our qRT-PCR data showed that *Car8*, *Car11*, and *Car12* were also expressed at moderate levels during inner ear development (Fig. 1C), while the remaining isozymes (*Car4*, *Car5a*, *Car5b*, *Car6*, *Car7*, *Car9*, *Car10*, and *Car15*) were expressed at undetectable or extremely low levels (Fig. 1D).

*Car3* was strongly expressed in the inner ears throughout developmental stages, suggesting an important role of *Car3* in inner ear development and function. Interestingly, acatalytic CA-RPs, such as *Car8* and *Car11*, were also expressed at moderate levels in developing inner ears, although *Car8* became undetectable in the mature inner ear at P21 (Fig. 1C). These results suggest that CA isozymes may play specific roles in different stages of inner ear development.

## Spatial Expression Patterns of Carbonic Anhydrases During Inner Ear Development

The localization of expression for each CA transcript was determined by in situ hybridization in developing (E15.5, P0, P5) and mature (P21) inner ears.

### *Abundant cytosolic isozymes,* Car1 *and* Car2

Consistent with qRT-PCR results (Fig. 1), *Car1* transcripts were barely detectable in the inner ear during embryonic and postnatal development (E15.5, P0, and P5; data not shown) and were present in the bone marrow of the otic capsule at P21 (Fig. 2A–A″, arrows). Recently, it has been shown that CAI is associated with ankylosing spondylitis, characterized by abnormal bone formation, in humans and CAI function is involved in bone formation in vitro (Chang et al., 2012).

*Car2* transcripts were expressed in mesenchymal cells adjacent to the stria vascularis, spiral limbus, and basilar membrane (Fig. 2B). Weak *Car2* expression was also present in epithelial cells in the outer sulcus and greater epithelial ridge (GER) (Fig. 2B′,B″, bracket and arrowhead). This broad *Car2* expression continued during neonatal development (Fig. 2E), but by P21, *Car2* expression was mainly present in type II and IV otic fibrocytes (Fig. 2D′, bracket) and bone marrow of the otic capsule (Fig. 2D′, white arrows). Weaker *Car2* expression was present in type I fibrocytes, the apical and basal margins of stria vascularis (arrowheads), and outer hair cells in the organ of Corti (asterisk) at P21. In the vestibules, weak and broad *Car2* expression was present in mesenchymal tissues surrounding the sensory organs at E15.5 (Fig. 2B, bracket), and stronger expression in the otic capsule at P5, and bone marrows at P21 (Fig. 2D, brackets).

Previously, CAII immunoreactivity has been detected in type I, III, and IV otic fibrocytes in the spiral ligament of the gerbil cochlea (Spicer and Schulte, 1991) and in type I, II, and IV fibrocytes in guinea pigs (Ichimiya et al., 1994). These expression patterns differ slightly from our results, which show strong *Car2* expression in type II and IV fibrocytes (Fig. 2). This difference could be due to different species or detection methods.

### *Potential role of* Car3 *as a free radical scavenger in otic fibrocytes*

Initially, *Car3* expression was closely associated with prospective type I otic fibrocytes at E15.5 (Fig. 2F,F′, asterisk), but gradually expanded to the entire spiral ligament, encompassing all types of otic fibrocytes by P5 (Fig. 2G,G′), and later restricted to type I, III, and V otic fibrocytes at P21 (Fig. 2H,H′, asterisk). Interestingly, *Car3* expression in the cochlear lateral wall at P21 was complementary to *Car2*, that is *Car3* was more abundant in type I and III fibrocytes while *Car2* was stronger in type II and IV fibrocytes (Fig. 2D′,H′, asterisk and brackets). Weak *Car3* expression was also detected in the otic capsule (Fig. 2G′,H′, arrows) and bony modiolus area at P5 (Fig. 2G,I, arrows), which disappeared by P21 (Fig. 2H, arrow). *Car3* expression was also present in the vestibular mesenchymal regions throughout development (Fig. 2F–H, brackets). Consistent with our data, CAIII immunoreactivity was also present in type I and III fibrocytes from human and gerbil cochlea (Spicer and Schulte, 1991; Weber et al., 2001).

Unlike the other isozymes, CAIII has relatively little CA activity (Sanyal et al., 1982; Engberg et al., 1985), but mainly functions as an oxy-radical scavenger and protects cells from oxidative damage by S-glutathiolation on two cysteine residues in response to oxidative stress (Raisanen et al., 1999; Mallis et al., 2002, 2000; Gailly et al., 2008). Nevertheless, introducing CAIII into hepatocellular carcinoma cells accelerated the speed at which culture medium was acidified, suggesting that CAIII can still catalyze carbon dioxide hydration, although at a reduced rate (Dai et al., 2008). The in vivo function of CAIII is unclear because *Car3* null mutants do not display obvious anatomical or physiological abnormalities (Kim et al., 2004). A recent study, however, showed that a lack of CAIII function attenuates ATP synthesis by mitochondria in skeletal muscle, although its underlying mechanism is unclear (Liu et al., 2007). Therefore, CAIII may play dual roles in otic fibrocytes: facilitating mitochondrial ATP synthesis as well as detoxifying free radicals resulting from active ATP synthesis.

### *Possible Functional Association of* Car12 *and* Car13 *With* Pendrin

*Car12* was expressed at P0 in regions that would become the outer sulcus and spiral prominence (Fig. 3A,A′, bracket). By P5, *Car12* expression in the outer sulcus had expanded to the associated root cell processes, continuing to P21 (Fig. 3B,I, brackets). *Car12* was also expressed in the endolymphatic duct at E15.5 (Fig. 3C). These *Car12* expression patterns closely overlap with expression of *Pendrin*, an anion exchanger that transports $Cl^-$, $I^-$, formate, and $HCO_3^-$ (Fig. 3D–F) (Everett et al., 1999; Wangemann et al., 2004). *Car12* was also weakly expressed in the spiral ganglion in the postnatal cochlea (Fig. 3A, arrows; data not shown) and also in Boettcher's cells at P21 (Fig. 3I, arrow). In addition, *Car12* was strongly expressed in the vestibular

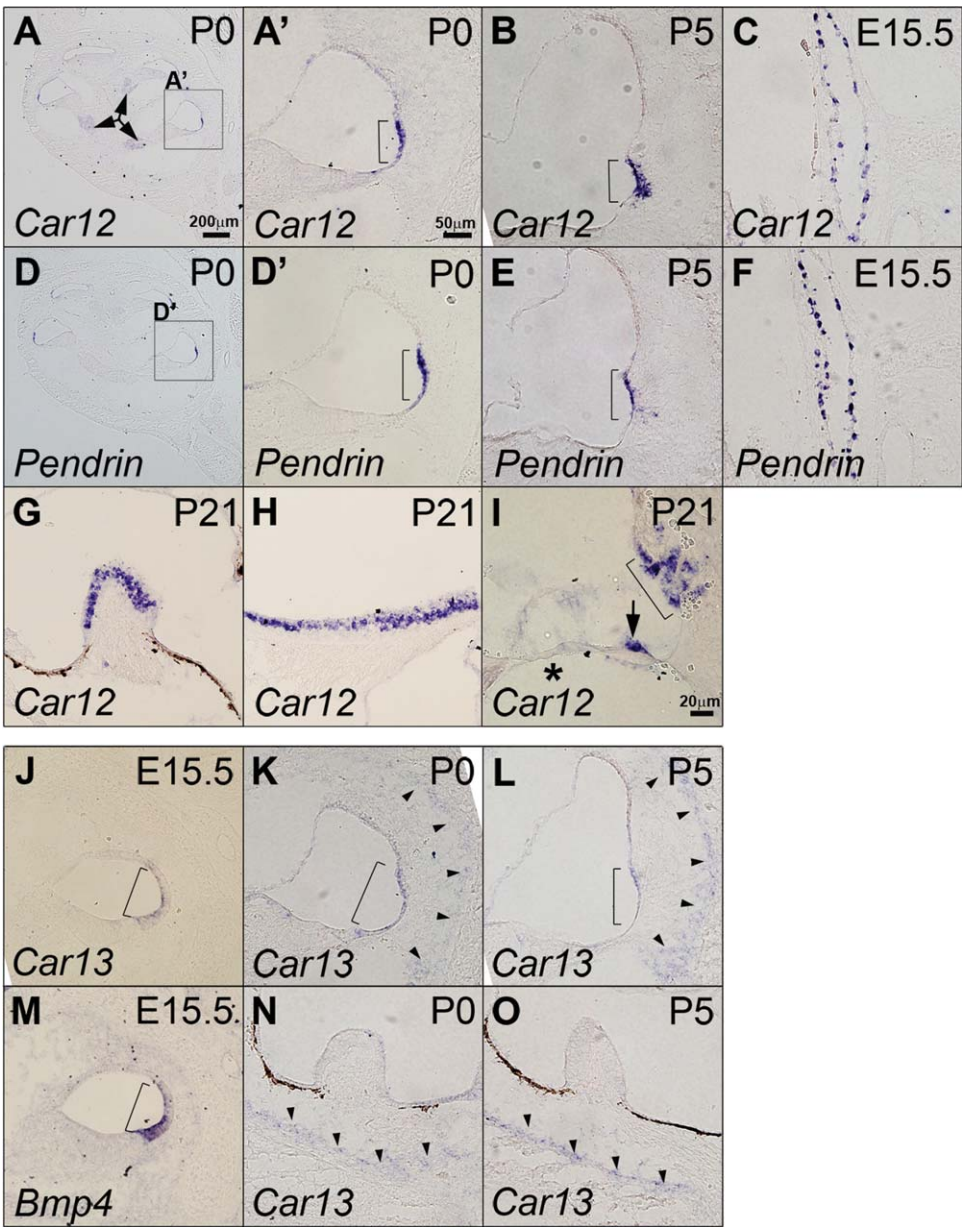


**Fig. 3.** Expression of *Car12* and *Car13* in the developing mouse inner ear. **A,B:** *Car12* was expressed in the spiral prominence and associated root cell processes (brackets) and also in the spiral ganglion (arrows). **C:** *Car12* was expressed in the endolymphatic duct at embryonic day (E) 15.5. **D–F:** *Car12* expression closely overlapped with *Pendrin*. **G–I:** At P21, *Car12* was expressed in the spiral prominence and associated root cell processes (I, bracket). In addition, *Car12* was also expressed in hair cells of cristae (G) and maculae (H) and Boettcher's cells (I, arrow), but not in hair cells of organ of Corti in the P21 cochlea (I, asterisk). **J–M:** *Car13* was weakly expressed on the lateral side of the lesser epithelial ridge (LER) (brackets), similar to *Bmp4* (M) at E15.5. *Car13* was also expressed in the spiral prominence and presumptive outer sulcus during neonatal development (brackets). **N,O:** *Car13* was weakly expressed in prospective type III fibrocytes during neonatal stages (K,L, arrowheads) and in the mesenchymal tissues along the otic capsule at E15.5 and P5 (N,O, arrowheads). Scale bar in A applies to D; the scale bar in A′ applies to B–C, D′, E–H, and J–O.

hair cells of cristae and maculae (Fig. 3G,H), but not in the auditory hair cells of the organ of Corti in the cochlea (Fig. 3I, asterisk).

*Car13* transcripts were observed in the lesser epithelial ridge (LER) area of E15.5 cochlea, which closely overlaps with *Bmp4* expression (Fig. 3J,M, brackets) (Hwang et al., 2010). At P0, *Car13* expression was restricted to the epithelial cells of the spiral prominence and outer sulcus, with faint expression in prospective type III fibrocytes (Fig. 3K, bracket, arrowheads), which was maintained until P21 (Fig. 3L, bracket and arrowheads; data not shown). In the vestibule, weak *Car13* expression was observed in the mesenchymal tissues along the otic capsule at E15.5 and P5, which is similar with the *Car13* expression pattern in the type III fibrocytes of the cochlea (Fig. 3K,L,N,O, arrows).

Previously, cytosolic and membrane-bound CAs have been shown to associate directly with ion transporters, forming a membrane protein complex called a biocarbonate transport metabolon. This complex can

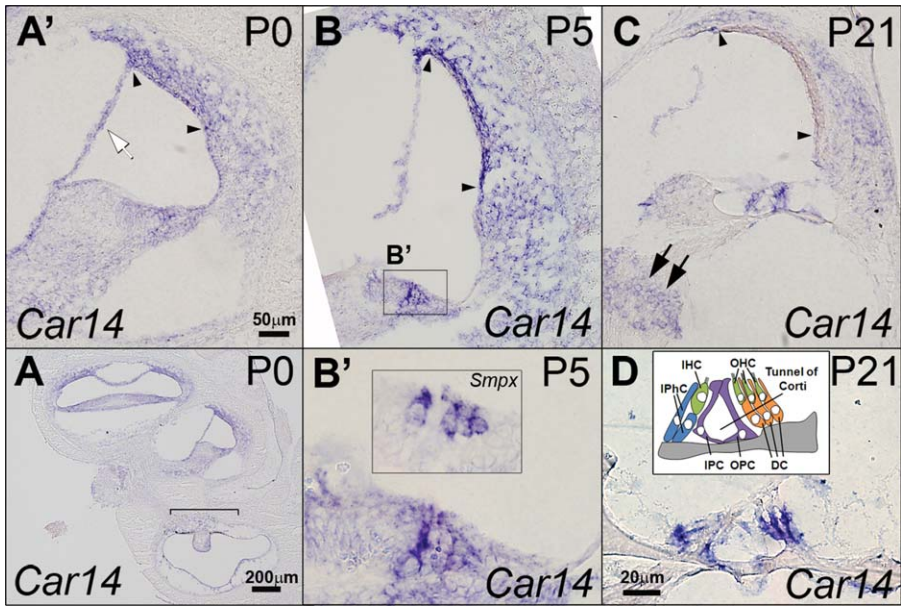


**Fig. 4.** Expression of *Car14* in the developing mouse cochlea. **A–C:** *Car14* was broadly expressed in both epithelial and mesenchymal tissues in the cochlea and vestibule during embryonic and neonatal development. *Car14* expression in the otic fibrocytes, Reissner's membrane (A′, white arrow), and stria vascularis (A′–C, arrowheads) at postnatal day (P) 0 and P5 became weaker at P21. *Car14* was also expressed in the organ of Corti in pillar cells and Deiters' cells at P5 (B,B′). The inset in B′ showed *Smpx* expression in the hair cells. At P21, *Car14* was expressed in the inner phalangeal cells, inner pillar cells, and Deiters' cells (C,D). The inset in D illustrates various cell types in the organ of Corti for comparison with the *Car14* expression domains. *Car14* was also weakly expressed in the spiral ganglion (C, arrows). The scale bar in A applies to B and C; the scale bar in D applies to B′.

significantly enhance $H^+/HCO_3^-$ transport by mass CA action supplying and dissipating the reaction products (Alvarez et al., 2003; Purkerson and Schwartz, 2007). For example, in the renal tube, a cytosolic CAII and a membrane-bound CAIV form transport metabolons with bicarbonate transporters such as AE1, NBC1, NBC3, and SCL26A6 and a proton antiporter such as NHE1 (Purkerson and Schwartz, 2007).

Based on expression of the transcripts of membrane-bound *Car12*, cytosolic *Car13*, and the anion exchanger *Pendrin* in the outer sulcus and root cell processes, it is possible that CAXII and CAXIII may physically associate with Pendrin or other transporters to form metabolons in the outer sulcus and root cell processes and regulate ion and pH homeostasis of endolymphatic fluid. Consistently, the unique biochemical properties of CAXIII, which catalyzes $CO_2$ hydration even in the presence of high $HCO_3^-$ concentrations, suggests that CAXIII may form metabolons in tissues that require tight bicarbonate regulation. For example, the female reproductive tract requires an alkaline environment to maintain sperm motility (Innocenti et al., 2004). Further experiments should examine whether CAXII and CAXIII indeed physically or functionally associate with Pendrin to regulate endolymph homeostasis.

### *A membrane-bound isozyme* Car14

*Car14* was broadly expressed in both epithelial and mesenchymal tissues in the cochlea at P0 (Fig. 4A,A′). At P5, *Car14* expression was stronger in the otic fibrocytes, stria vascularis, and supporting cells in the organ of Corti (Fig. 4B,B′). *Car14* expression was maintained in the otic fibrocytes and greatly reduced in the stria vascularis at P21 (Fig. 4C). *Car14* expression in Reissner's membrane at P0 decreased by P5 (Fig. 4A′,B, white arrow). *Car14* expression in the organ of Corti at P5 appeared to be in pillar cells and Deiters' cells when compared with *Smpx*, a hair cell-specific gene (Fig. 4B′) (Yoon et al., 2011). At P21, *Car14* expression was observed in the inner phalangeal cells and inner pillar cells located at the medial side of the tunnel of Corti, and three Deiters' cells at the lateral side but not in the outer pillar cells (Fig. 4D). *Car14* was also weakly expressed in the spiral ganglion region (Fig. 4C, arrows). In the vestibule, weak *Car14* expression was broadly observed in the mesenchymal tissues in the vestibule, but not in the otic capsule (Fig. 4A, bracket).

It was shown in the kidney that the membrane-bound CAXIV (in rodents; CAIV in humans) is expressed on the luminal surface of the renal tube and facilitates bicarbonate and fluid transport by ion transporters such as NBCI (Alvarez et al., 2003; Purkerson and Schwartz, 2007). Previously, it has been suggested that $CO_2$ in the outer hair cells is hydroxylated by means of intracellular CA in the outer hair cells, and exchanged to the endolymph or diffused to the region between the outer hair cells and Deiters' cells (Thalmann et al., 1970; Kimura, 1975; Ikeda et al., 1992; Okamura et al., 1996). Thus, it is also possible that CAII expressed in the outer hair cells may cooperate with CAXIV expressed on the extracellular surface of Deiters' cells to facilitate the hydroxylation and transport of $CO_2$, which is the major product of high cellular metabolism in the hair cells, and play roles in optimal pH regulation and fluid homeostasis in the organ of Corti.

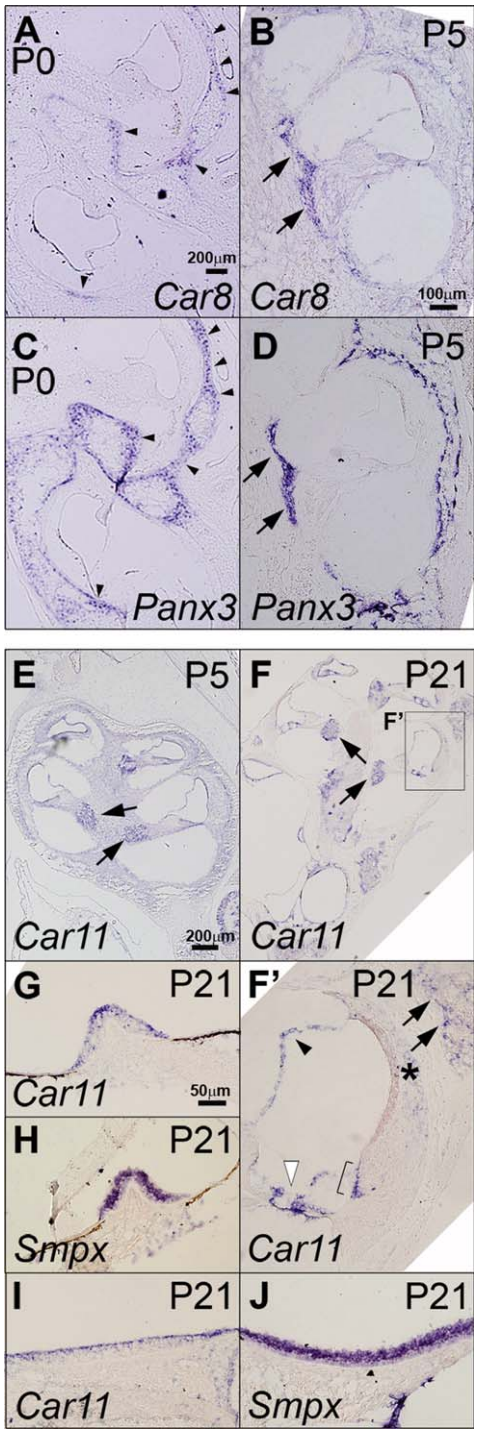


**Fig. 5.** Expression of *Car8* and *Car11* in the developing mouse inner ear. **A,B:** *Car8* was first detected at postnatal day (P) 0 in the otic capsule by the basal turn of the cochlear duct and in the vestibule (A, arrowheads). At P5, *Car8* expression in the otic capsule was down-regulated but instead expressed in the modiolus (arrows). **C,D:** *Panx3* expression indicates prehypertrophic chondrocytes at P0 (C, arrowheads) and osteoblasts at P5 (D, arrows). **E,F:** *Car11* was broadly expressed in both epithelial and mesenchymal tissues of the inner ear and also in the spiral ganglion at P5 (E, arrows). **F,F′**: At P21, *Car11* was expressed in a similar broad pattern in the spiral ganglion (F, arrows), Reissner's membrane (black arrowhead), organ of Corti (white arrowhead), bone marrow of the otic capsule (F′, arrows), and spiral prominence and the associated root cell processes (bracket). *Car11* was also weakly expressed in type I fibrocytes (F′, asterisk). **G,I:** Supporting cells in the cristae and maculae expressed *Car11* at P21. **H,J:** *Smpx* was expressed in the hair cells of cristae and maculae at P21. Scale bar in A applies to C, the scale bar in B applies to D, the scale bar in E applies to F, and the scale bar in G applies to F′ and H–J.

### *Acatalytic CA-related proteins* Car8 *and* Car11

An acatalytic CA-RP, *Car8*, was first detected at P0 in the otic capsule near the basal turn of the cochlear duct and of the vestibule (Fig. 5A, arrowheads). This expression overlaps with *Pannexin 3* (*Panx3*), which is expressed in the prehypertrophic chondrocytes, perichondrium, and osteoblasts (Fig. 5C, arrowheads) (Iwamoto et al., 2010). At P5, *Car8* expression in the otic capsule was down-regulated, and was expressed instead in the modiolus, which overlaps with *Panx3* (Fig. 5B,D, arrows). *Car8* transcripts were not detected in the inner ear at P21, consistent with the qRT-PCR results (Fig. 1). Based on the developmental stage and ossification pattern, it appears that *Car8* is expressed in prehypertrophic chondrocytes in the otic capsule at P0, and later is expressed in differentiating osteoblasts in the modiolus.

It is interesting that *Car8* expression in the developing otic capsule and modiolus overlaps with *Panx3*, which is induced in prehypertrophic chondrocytes and promotes chondrocyte and osteoblast differentiation. *Panx3* performs these roles as a $Ca^{2+}$ channel in the endoplasmic reticulum (ER), as a hemichannel releasing ATP into the extracellular space, and as a gap junction propagating $Ca^{2+}$ waves between cells (Iwamoto et al., 2010; Ishikawa et al., 2011). *Panx3* as an ER $Ca^{2+}$ channel was activated similar to Inositol trisphosphate 3 receptors (IP3Rs), which increase intracellular $Ca^{2+}$ levels upon IP3 binding to and activating IP3Rs. Interestingly, *Car8* was shown to reduce the affinity of IP3Rs for IP3 and inhibit increases in intracellular calcium (Hirota et al., 2003). Thus, it is possible that CAVIII plays a role in forming the otic capsule and modiolus by modulating IP3-induced $Ca^{2+}$ release during osteoblast differentiation. Although this hypothesis remains to be tested, *Car8* expression in the differentiating otic capsule and modiolus is interesting because only *Car1* and *Car2*, which are expressed in bone marrow cells in otic capsule, have been known as major carbonic anhydrases associated with bone development (Lehenkari et al., 1998; Rajachar et al., 2009).

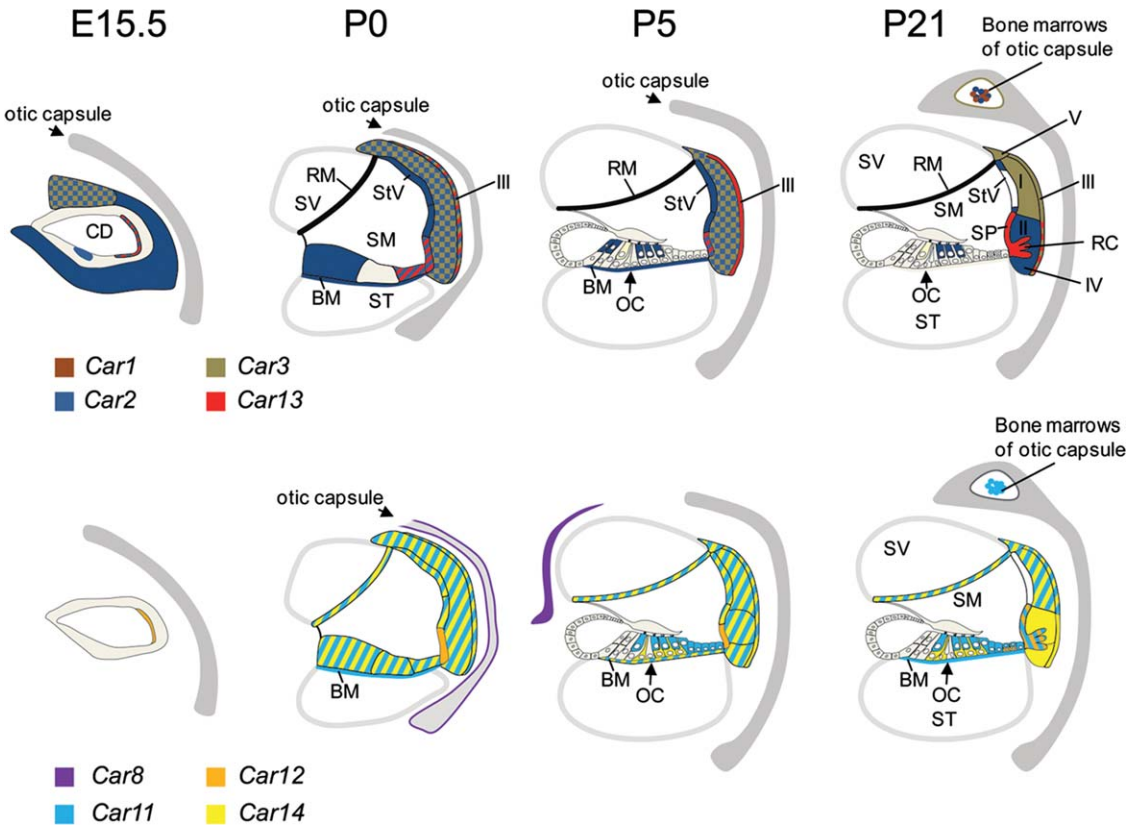


**Fig. 6.** A schematic diagram summarizing carbonic anhydrase isozyme expression during inner ear development. Transcripts of each CA isozyme are illustrated at each developmental stage from embryonic day (E) 15.5 to postnatal (P) 21. Please refer to the text for details. CD, cochlear duct; StV, stria vascularis; SV, scala vestibule; SM, scala media; ST, scala tympani; BM, basilar membrane; RM, Reissner's membrane; OC, organ of Corti; SP, spiral prominence; RC, root cell processes; I, type I fibrocyte; II, type II fibrocyte; III, type III fibrocyte; IV, type IV fibrocyte; V, type V fibrocyte.

Another CA-RP, *Car11*, was broadly expressed in the inner ear at P5, with slightly stronger expression in the spiral ganglion (Fig. 5E, arrows). At P21, *Car11* was expressed in the spiral ganglion (Fig. 5F, arrows), Reissner's membrane (Fig. 5F′, black arrowhead), organ of Corti (Fig. 5F′, white arrowhead), bone marrow of the otic capsule (Fig. 5F′, arrows), spiral prominence, and root cell processes (Fig. 5F′, bracket). *Car11* was also weakly expressed in type I otic fibrocytes (Fig. 5F′, asterisk). In the vestibule, *Car11* expression was observed in the apical portion of cristae and maculae, most likely in the supporting cells, based on the comparison with the hair cell specific expression of *Smpx* (Fig. 5G–J). Although CAXI immunoreactivity has been shown in the developing and mature human brain (Taniuchi et al., 2002) and in gastrointestinal stromal tumors (Morimoto et al., 2005), the physiological roles of *Car11* in the mouse inner ear remains to be elucidated.

## Conclusions

In this study, we systemically surveyed the expression patterns of transcripts for all 16 known mammalian CA isozymes throughout mammalian inner ear development. Our data show that not all isozymes are expressed, and each isozyme has unique temporal and spatial expression patterns during inner ear development, which are summarized in Figure 6. The expression patterns for some isozymes closely overlapped with genes previously associated with inner ear development or function, such as *Pendrin*, *Pou3f4*, or *Bmp4*. In addition, we also profiled the expression patterns of CA isozymes in other organs, such as brain, kidney, and liver from P21 mice, showing that each organ expresses a unique combination of CA isozymes, although some isozymes, such as *Car2* and *Car14*, appear to be expressed ubiquitously (Fig. 1). These expression patterns suggest that each CA isozyme plays a unique role in mammalian development and function depending on its temporal and spatial expression pattern.

## EXPERIMENTAL PROCEDURES

### Tissue Dissection, RNA Isolation, and cDNA Synthesis

All animals were handled according to the guidelines for the Care and Use of Laboratory Animals of Yonsei University College of Medicine. The protocol for obtaining inner ear samples was approved by the Committee on Animal Research at Yonsei University College of Medicine. The entire inner ear tissues including the vestibule and cochlea as well as surrounding otic capsule were dissected at all stages examined. Total RNA was extracted using the RNeasy Mini kit (Qiagen, Hilden, Germany) from inner ear, brain, kidney, and liver tissues dissected from C57BL/6 mice.

**TABLE 1. Primer Sequences for Quantitative Real-Time PCR**

| Gene | Forward primer (5′-3′) | Reverse primer (5′-3′) | Product size(bp) cDNA | Product size(bp) gDNA |
|---|---|---|---|---|
| *Gapdh* | GGTGCTGAGTATGTCGTGGA | CTAAGCAGTTGGTGGTGCAG | 202 | 300 |
| *Car1* | GCAAGTGCAGACTGGGGATA | TGGAAAGAATGTCCCACGTT | 200 | 621 |
| *Car2* | TGAAAGGAGGACCCCTCAGT | AATACCCAAAACAGCCAATCC | 200 | 594 |
| *Car3* | GAGAAAGGCGAGTTCCAGATT | AGCTCACAGTCATGGGCTCT | 202 | 946 |
| *Car4* | CTTCATCCTCGTCGGCTATG | ATGGCAAAGTGTCTCCCATC | 204 | 803 |
| *Car5a* | GCCTCTGGGAAACCACTACA | TTCAGAAACACGCCGATGAC | 201 | 3421 |
| *Car5b* | ACAGAAATTGGTGGACACTTTG | CTGGTCACGGTCAACCTCAA | 196 | 1292 |
| *Car6* | CCCCTGAGCTTGGTGAACTA | TGATCCCATCAATGGTGTGT | 202 | 834 |
| *Car7* | ACCTATCCTGGCTCCCTGAC | AAGGATGCTTTGACCACTCG | 203 | 667 |
| *Car8* | GGAACATGTTGGCTTGAAGG | AAAGGGTATCGGAATAATATCCA | 198 | 2359 |
| *Car9* | ATCACCCAGGCTCAGAACAC | TTTCTTCCAAATGGGACAGC | 198 | 1266 |
| *Car10* | TCACTTATGATGGGTCGATGA | TGGTGCGAATACAGCGATTA | 201 | 2157 |
| Car11 | TCTCCTTCCTACCTGCATCC | GCAGCACTGAGGTTCCCATA | 202 | 415 |
| *Car12* | CGCCAATCCATCATATGACAA | GAAATCTGCACAGGGTTTCG | 204 | 484 |
| *Car13* | TGCATGTTGTCCACTGGAAT | AGCAAGCATAACGGGTCAAA | 202 | 2068 |
| *Car14* | GCTACAACGGCTCACTCACA | AAGCAAAGATGGTCCTCTGG | 198 | 284 |
| *Car15* | CGGTGCTCTGGACTGTCTTT | GGGCAGGGTAGAGACTGATG | 203 | 299 |

RNase-free DNase was used to digest of genomic DNA during RNA purification (Qiagen, Hilden, Germany). The concentration and purity of the extracted RNAs were determined using both the spectrophotometric method at 260 and 280 nm and RNA electrophoresis. One microgram of total RNA was subjected to reverse transcription with oligod$(T)_{19}$ primer using the High Capacity cDNA Reverse Transcription Kit (Applied Biosystems, Foster City, CA).

## Semi-quantitative Reverse Transcription PCR Analysis

Synthesized cDNAs were subjected to semi-quantitative RT-PCR to analyze relative expression levels of CA isozymes among tissues. CA isozyme specific PCR primers previously reported were used for RT-PCR (Lacruz et al., 2010). PCR conditions were as follows: 28 cycles of denaturation at 94°C for 20 sec, annealing at 55°C for 40 sec, and extension at 72°C for 40 sec. The first denaturation step and the last extension step were performed at 95°C for 15 min and 72°C for 5 min, respectively. PCR products were separated and visualized on a 2% agarose gel.

## Quantitative Real-Time PCR

qRT-PCR was performed to analyze the expression of each CA isozyme during inner ear development at E15.5, P0, P5, and P21. RNA purified from three replicates of each inner ear sample was used for qRT-PCR. PCR primers were designed based on mRNA sequences in the GenBank database (Table 1). Forward and reverse primers from each primer set were designed from different exons to distinguish transcripts from genomic DNA. *GAPDH* (glyceraldehyde-3-phosphate dehydrogenase) was used as an internal control for normalization. qRT-PCR for each CA isozyme was performed in triplicate using SYBR Green PCR Master Mix and the Applied Biosystems StepOnePlus Real-Time PCR Systems (Applied Biosystems). A melting curve analysis was always performed after the amplification to check PCR specificity. The results were analyzed by StepOne Software v2.1 (Applied Biosystems). The normalization and relative quantification were calculated using $2^{-\Delta\Delta Ct}$ method (Livak and Schmittgen, 2001).

## In Situ Hybridization

For E15.5 embryos and neonatal (P0 and P5) pups, animals were killed by decapitation and then hemi-sectioned. After removing the brain, the specimens were fixed in 4% paraformaldehyde in phosphate buffered saline (PBS) overnight at 4°C, dehydrated in 30% sucrose in PBS overnight at 4°C, embedded in OCT compound (Sakura, Tokyo, Japan), and stored at −80°C until use. For P21 mice, the entire inner ear tissues including the otic capsule were dissected. For better penetration of fixatives, parts of the semicircular canals were cut off, the oval and round windows were opened up, and the apex of the cochlea was punctured. After overnight fixation, the specimens were decalcified in 0.2 M EDTA in DEPC-PBS at 4°C for 2 days, followed by dehydration and mounting. Tissues were sectioned at 12 μm thickness for in situ hybridization, which was performed as previously described (Morsli et al., 1998). At least three animals were tested for each CA isozyme at each developmental stage. Sense RNA probes were also included as controls, which showed no signal anywhere in the inner ear.

Probes for *Bmp4* (Morsli et al., 1998), *Pou3f4* (Phippard et al., 1998), *Smpx* (Yoon et al., 2011), and *Pendrin* (Everett et al., 1999) were prepared as previously described. RNA probes for *Car1* were generated from a 381 base pair (bp) mouse *Car1* cDNA containing the +594 to +786 coding region and the 188 bp 3′ untraslated region (NM_009799.4); for *Car2*, from a 410 bp mouse *Car2* cDNA containing the +654 to +783 coding region and the 280 bp 3′untranslated region (NM_009801.4); for *Car3*, from a 404

bp mouse *Car3* cDNA containing the +687 to +783 coding region and the 334 bp 3′ untranslated region (NM_007606.3); for *Car8*, from a 621 bp mouse *Car8* cDNA containing the +212 to +832 coding region and the 12 bp 5′ untranslated region (NM_007592.3); for *Car12*, from a 471 bp mouse *Car12* cDNA containing the +947 to +1,065 coding region and the 352 bp 5′ untranslated region (NM_178396.4); for *Car13*, from a 404 bp mouse *Car13* cDNA containing the +664 to +789 coding region and the 278 bp 5′ untranslated region (NM_024495.5); for *Car14*, from a 856 bp mouse *Car14* cDNA containing the +1 to +821 coding region and the 35 bp 5′ untranslated region (NM_011797.2); for *Car11*, from a 916 bp mouse *Car11* cDNA containing 634 bp coding region and the 282 bp 5′ untranslated region (NM_009800.4); for *Osteocalcin,* from a 33 bp mouse *Osteocalcin* cDNA containing the 47 bp 5′ untranslated region and the entire open reading frame (NM_007541.2); for *Pannexin3*, from a 559 bp mouse *Pannexin3* cDNA containing the +565 to +1,123 coding region (NM_172454.2).

## REFERENCES


Alvarez BV, Loiselle FB, Supuran CT, Schwartz GJ, Casey JR. 2003. Direct extracellular interaction between carbonic anhydrase IV and the human NBC1 sodium/bicarbonate co-transporter. Biochemistry 42:12321–12329.

Chang X, Zheng Y, Yang Q, Wang L, Pan J, Xia Y, Yan X, Han J. 2012. Carbonic anhydrase I is involved in the process of bone formation and is susceptible to ankylosing spondylitis. Arthritis Res Ther 14:R176.

Chiche J, Ilc K, Laferriere J, Trottier E, Dayan F, Mazure NM, Brahimi-Horn MC, Pouyssegur J. 2009. Hypoxia-inducible carbonic anhydrase IX and XII promote tumor cell growth by counteracting acidosis through the regulation of the intracellular pH. Cancer Res 69:358–368.

Dai HY, Hong CC, Liang SC, Yan MD, Lai GM, Cheng AL, Chuang SE. 2008. Carbonic anhydrase III promotes transformation and invasion capability in hepatoma cells through FAK signaling pathway. Mol Carcinog 47:956–963.

Engberg P, Millqvist E, Pohl G, Lindskog S. 1985. Purification and some properties of carbonic anhydrase from bovine skeletal muscle. Arch Biochem Biophys 241:628–638.

Erulkar SD, Maren TH. 1961. Carbonic anhydrase and the inner ear. Nature 189:459–460.

Esbaugh AJ, Tufts BL. 2006. The structure and function of carbonic anhydrase isozymes in the respiratory system of vertebrates. Respir Physiol Neurobiol 154:185–198.

Everett LA, Morsli H, Wu DK, Green ED. 1999. Expression pattern of the mouse ortholog of the Pendred's syndrome gene (Pds) suggests a key role for pendrin in the inner ear. Proc Natl Acad Sci U S A 96:9727–9732.

Gailly P, Jouret F, Martin D, Debaix H, Parreira KS, Nishita T, Blanchard A, Antignac C, Willnow TE, Courtoy PJ, Scheinman SJ, Christensen EI, Devuyst O. 2008. A novel renal carbonic anhydrase type III plays a role in proximal tubule dysfunction. Kidney Int 74:52–61.

Henry RP, Swenson ER. 2000. The distribution and physiological significance of carbonic anhydrase in vertebrate gas exchange organs. Respir Physiol 121:1–12.

Hirota J, Ando H, Hamada K, Mikoshiba K. 2003. Carbonic anhydrase-related protein is a novel binding protein for inositol 1,4,5-trisphosphate receptor type 1. Biochem J 372:435–441.

Hsu CJ, Nomura Y. 1985. Carbonic anhydrase activity in the inner ear. Acta Otolaryngol Suppl 418:1–42.

Hwang CH, Guo D, Harris MA, Howard O, Mishina Y, Gan L, Harris SE, Wu DK. 2010. Role of bone morphogenetic proteins on cochlear hair cell formation: analyses of Noggin and Bmp2 mutant mice. Dev Dyn 239:505–513.

Ichimiya I, Adams JC, Kimura RS. 1994. Immunolocalization of Na+, K(+)-ATPase, Ca(++)-ATPase, calcium-binding proteins, and carbonic anhydrase in the guinea pig inner ear. Acta Otolaryngol 114:167–176.

Ikeda K, Kusakari J, Takasaka T, Saito Y. 1987. Early effects of acetazolamide on anionic activities of the guinea pig endolymph: evidence for active function of carbonic anhydrase in the cochlea. Hear Res 31:211–216.

Ikeda K, Saito Y, Nishiyama A, Takasaka T. 1992. Intracellular pH regulation in isolated cochlear outer hair cells of the guinea-pig. J Physiol 447:627–648.

Innocenti A, Lehtonen JM, Parkkila S, Scozzafava A, Supuran CT. 2004. Carbonic anhydrase inhibitors. Inhibition of the newly isolated murine isozyme XIII with anions. Bioorg Med Chem Lett 14:5435–5439.

Ishikawa M, Iwamoto T, Nakamura T, Doyle A, Fukumoto S, Yamada Y. 2011. Pannexin 3 functions as an ER Ca(2+) channel, hemichannel, and gap junction to promote osteoblast differentiation. J Cell Biol 193:1257–1274.

Iwamoto T, Nakamura T, Doyle A, Ishikawa M, de Vega S, Fukumoto S, Yamada Y. 2010. Pannexin 3 regulates intracellular ATP/cAMP levels and promotes chondrocyte differentiation. J Biol Chem 285:18948–19958.

Jarvela S, Parkkila S, Bragge H, Kahkonen M, Parkkila AK, Soini Y, Pastorekova S, Pastorek J, Haapasalo H. 2008. Carbonic anhydrase IX in oligodendroglial brain tumors. BMC Cancer 8:1.

Kido T, Sekitani T, Yamashita H, Endo S, Masumitsu Y, Shimogori H. 1991. Effects of carbonic anhydrase inhibitor on the otolithic organs of developing chick embryos. Am J Otolaryngol 12:191–195.

Kim G, Lee TH, Wetzel P, Geers C, Robinson MA, Myers TG, Owens JW, Wehr NB, Eckhaus MW, Gros G, Wynshaw-Boris A, Levine RL. 2004. Carbonic anhydrase III is not required in the mouse for normal growth, development, and life span. Mol Cell Biol 24:9942–9947.

Kimura RS. 1975. The ultrastructure of the organ of Corti. Int Rev Cytol 42:173–222.

Lacruz RS, Hilvo M, Kurtz I, Paine ML. 2010. A survey of carbonic anhydrase mRNA expression in enamel cells. Biochem Biophys Res Commun 393:883–887.

Lehenkari P, Hentunen TA, Laitala-Leinonen T, Tuukkanen J, Vaananen HK. 1998. Carbonic anhydrase II plays a major role in osteoclast differentiation and bone resorption by effecting the steady state intracellular pH and Ca2+. Exp Cell Res 242:128–137.

Lim DJ, Karabinas C, Trune DR. 1983. Histochemical localization of carbonic anhydrase in the inner ear. Am J Otolaryngol 4:33–42.

Liu M, Walter GA, Pathare NC, Forster RE, Vandenborne K. 2007. A quantitative study of bioenergetics in skeletal muscle lacking carbonic anhydrase III using 31P magnetic resonance spectroscopy. Proc Natl Acad Sci U S A 104:371–376.

Livak KJ, Schmittgen TD. 2001. Analysis of relative gene expression data using real-time quantitative PCR and the 2 (-Delta Delta C(T)) Method. Methods 25:402–408.

Mallis RJ, Hamann MJ, Zhao W, Zhang T, Hendrich S, Thomas JA. 2002. Irreversible thiol oxidation in carbonic anhydrase III: protection by S-glutathiolation and detection in aging rats. Biol Chem 383:649–662.

Mallis RJ, Poland BW, Chatterjee TK, Fisher RA, Darmawan S, Honzatko RB, Thomas JA. 2000. Crystal structure of S-glutathiolated carbonic anhydrase III. FEBS Lett 482:237–241.

Margolis DS, Szivek JA, Lai LW, Lien YH. 2008. Phenotypic characteristics of bone in carbonic anhydrase II-deficient mice. Calcif Tissue Int 82:66–76.

Morimoto K, Nishimori I, Takeuchi T, Kohsaki T, Okamoto N, Taguchi T, Yunoki S, Watanabe R, Ohtsuki Y, Onishi S. 2005. Overexpression of carbonic anhydrase-related protein XI promotes proliferation and invasion of gastrointestinal stromal tumors. Virchows Arch 447:66–73.

Morsli H, Choo D, Ryan A, Johnson R, Wu DK. 1998. Development of the mouse inner ear and origin of its sensory organs. J Neurosci 18:3327–3335.

Okamura HO, Sugai N, Suzuki K, Ohtani I. 1996. Enzyme-histochemical localization of carbonic anhydrase in the inner ear of the guinea pig and several improvements of the technique. Histochem Cell Biol 106:425–430.

Pan PW, Rodriguez A, Parkkila S. 2007. A systematic quantification of carbonic anhydrase transcripts in the mouse digestive system. BMC Mol Biol 8:22.

Parkkila AK, Scarim AL, Parkkila S, Waheed A, Corbett JA, Sly WS. 1998. Expression of carbonic anhydrase V in pancreatic beta cells suggests role for mitochondrial carbonic anhydrase in insulin secretion. J Biol Chem 273:24620–24623.

Phippard D, Heydemann A, Lechner M, Lu L, Lee D, Kyin T, Crenshaw EB, 3rd. 1998. Changes in the subcellular localization of the Brn4 gene product precede mesenchymal remodeling of the otic capsule. Hear Res 120:77–85.

Prazma J. 1978. Carbonic anhydrase in the generation of cochlear potentials. Am J Physiol 235:F317–F320.

Purichia N, Erway LC. 1972. Effects of dichlorophenamide, zinc, and manganese on otolith development in mice. Dev Biol 27:395–405.

Purkerson JM, Schwartz GJ. 2007. The role of carbonic anhydrases in renal physiology. Kidney Int 71:103–115.

Raisanen SR, Lehenkari P, Tasanen M, Rahkila P, Harkonen PL, Vaananen HK. 1999. Carbonic anhydrase III protects cells from hydrogen peroxide-induced apoptosis. FASEB J 13:513–522.

Rajachar RM, Tung E, Truong AQ, Look A, Giachelli CM. 2009. Role of carbonic anhydrase II in ectopic calcification. Cardiovasc Pathol 18:77–82.

Sanyal G, Swenson ER, Pessah NI, Maren TH. 1982. The carbon dioxide hydration activity of skeletal muscle carbonic anhydrase. Inhibition by sulfonamides and anions. Mol Pharmacol 22:211–220.

Shah GN, Ulmasov B, Waheed A, Becker T, Makani S, Svichar N, Chesler M, Sly WS. 2005. Carbonic anhydrase IV and XIV knockout mice: roles of the respective carbonic anhydrases in buffering the extracellular space in brain. Proc Natl Acad Sci U S A 102:16771–16776.

Sly WS, Hu PY. 1995. Human carbonic anhydrases and carbonic anhydrase deficiencies. Annu Rev Biochem 64:375–401.

Spicer SS, Schulte BA. 1991. Differentiation of inner ear fibrocytes according to their ion transport related activity. Hear Res 56:53–64.

Sterkers O, Saumon G, Tran Ba Huy P, Ferrary E, Amiel C. 1984. Electrochemical heterogeneity of the cochlear endolymph: effect of acetazolamide. Am J Physiol 246:F47–F53.

Supuran CT. 2008a. Carbonic anhydrases–an overview. Curr Pharm Des 14:603–614.

Supuran CT. 2008b. Carbonic anhydrases: novel therapeutic applications for inhibitors and activators. Nat Rev Drug Discov 7:168–181.

Taniuchi K, Nishimori I, Takeuchi T, Fujikawa-Adachi K, Ohtsuki Y, Onishi S. 2002. Developmental expression of carbonic anhydrase-related proteins VIII, X, and XI in the human brain. Neuroscience 112:93–99.

Thalmann I, Matschinsky FM, Thalmann R. 1970. Quantitative study of selected enzymes involved in energy metabolism of the cochlear duct. Ann Otol Rhinol Laryngol 79:12–29.

Tohse H, Ando H, Mugiya Y. 2004. Biochemical properties and immunohistochemical localization of carbonic anhydrase in the sacculus of the inner ear in the salmon Oncorhynchus masou. Comp Biochem Physiol A Mol Integr Physiol 137:87–94.

Wangemann P, Itza EM, Albrecht B, Wu T, Jabba SV, Maganti RJ, Lee JH, Everett LA, Wall SM, Royaux IE, Green ED, Marcus DC. 2004. Loss of KCNJ10 protein expression abolishes endocochlear potential and causes deafness in Pendred syndrome mouse model. BMC Med 2:30.

Weber PC, Cunningham CD III, Schulte BA. 2001. Potassium recycling pathways in the human cochlea. Laryngoscope 111:1156–1165.

Xu Y, Feng L, Jeffrey PD, Shi Y, Morel FM. 2008. Structure and metal exchange in the cadmium carbonic anhydrase of marine diatoms. Nature 452:56–61.

Yoon H, Lee DJ, Kim MH, Bok J. 2011. Identification of genes concordantly expressed with Atoh1 during inner ear development. Anat Cell Biol 44:69–78.